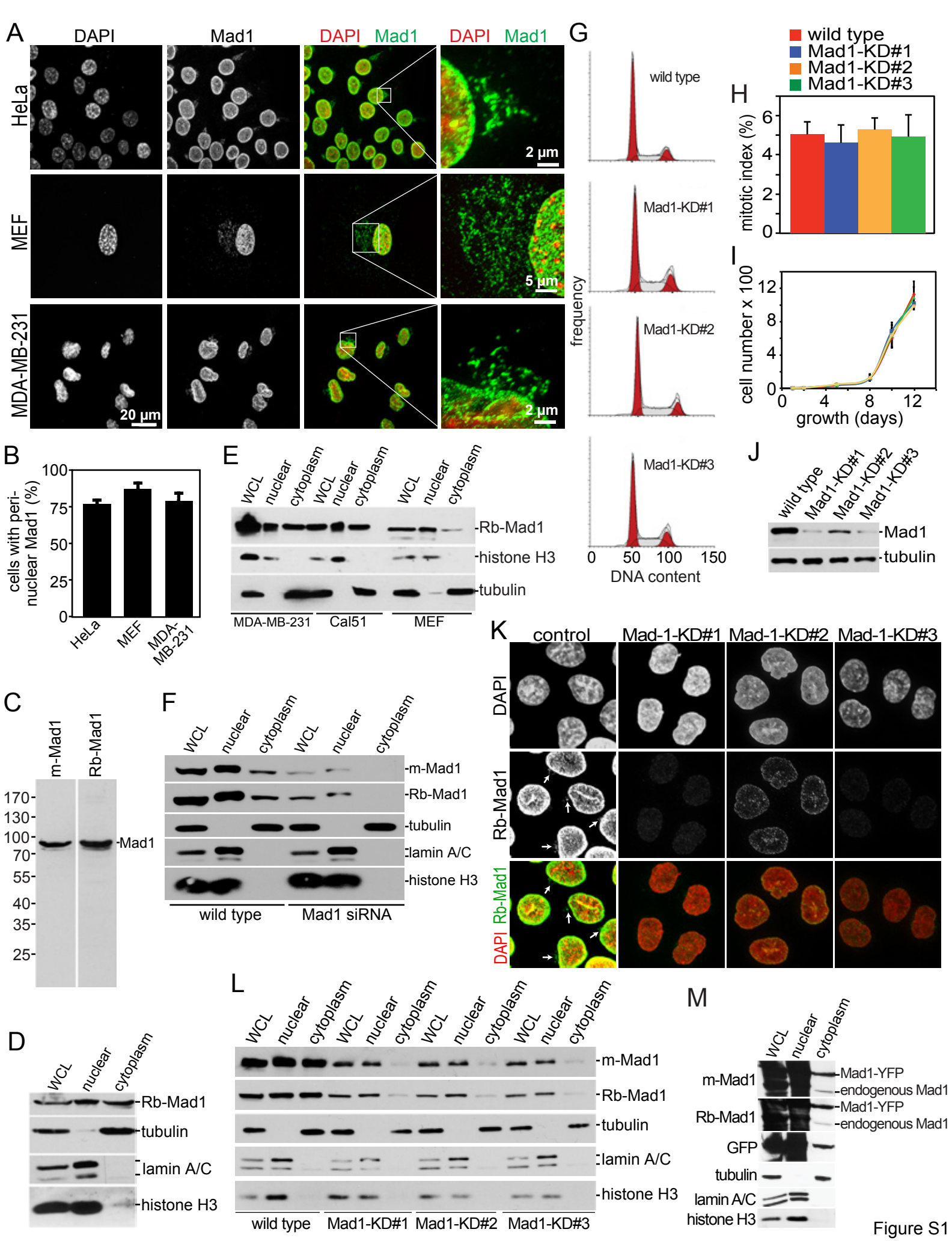
A
DAPI
Mad1
DAPI Mad1
DAPI Mad1
HeLa
MEF
MDA-MB-231
2 µm
5 µm
20 µm
2 µm
G
wild type
Mad1-KD#1
Mad1-KD#2
Mad1-KD#3
frequency
DNA content
H
mitotic index (%)
I
cell number x 100
growth (days)
B
cells with peri-nuclear Mad1 (%)
HeLa
MEF
MDA-MB-231
E
WCL
nuclear
cytoplasm
Rb-Mad1
histone H3
tubulin
MDA-MB-231
Cal51
MEF
J
wild type
Mad1-KD#1
Mad1-KD#2
Mad1-KD#3
Mad1
tubulin
C
m-Mad1
Rb-Mad1
Mad1
F
m-Mad1
Rb-Mad1
tubulin
lamin A/C
histone H3
wild type
Mad1 siRNA
K
control
Mad-1-KD#1
Mad-1-KD#2
Mad-1-KD#3
DAPI
Rb-Mad1
DAPI Rb-Mad1
D
WCL
nuclear
cytoplasm
Rb-Mad1
tubulin
lamin A/C
histone H3
L
m-Mad1
Rb-Mad1
tubulin
lamin A/C
histone H3
wild type
Mad1-KD#1
Mad1-KD#2
Mad1-KD#3
M
m-Mad1
Rb-Mad1
GFP
tubulin
lamin A/C
histone H3
Mad1-YFP
endogenous Mad1

Figure S1

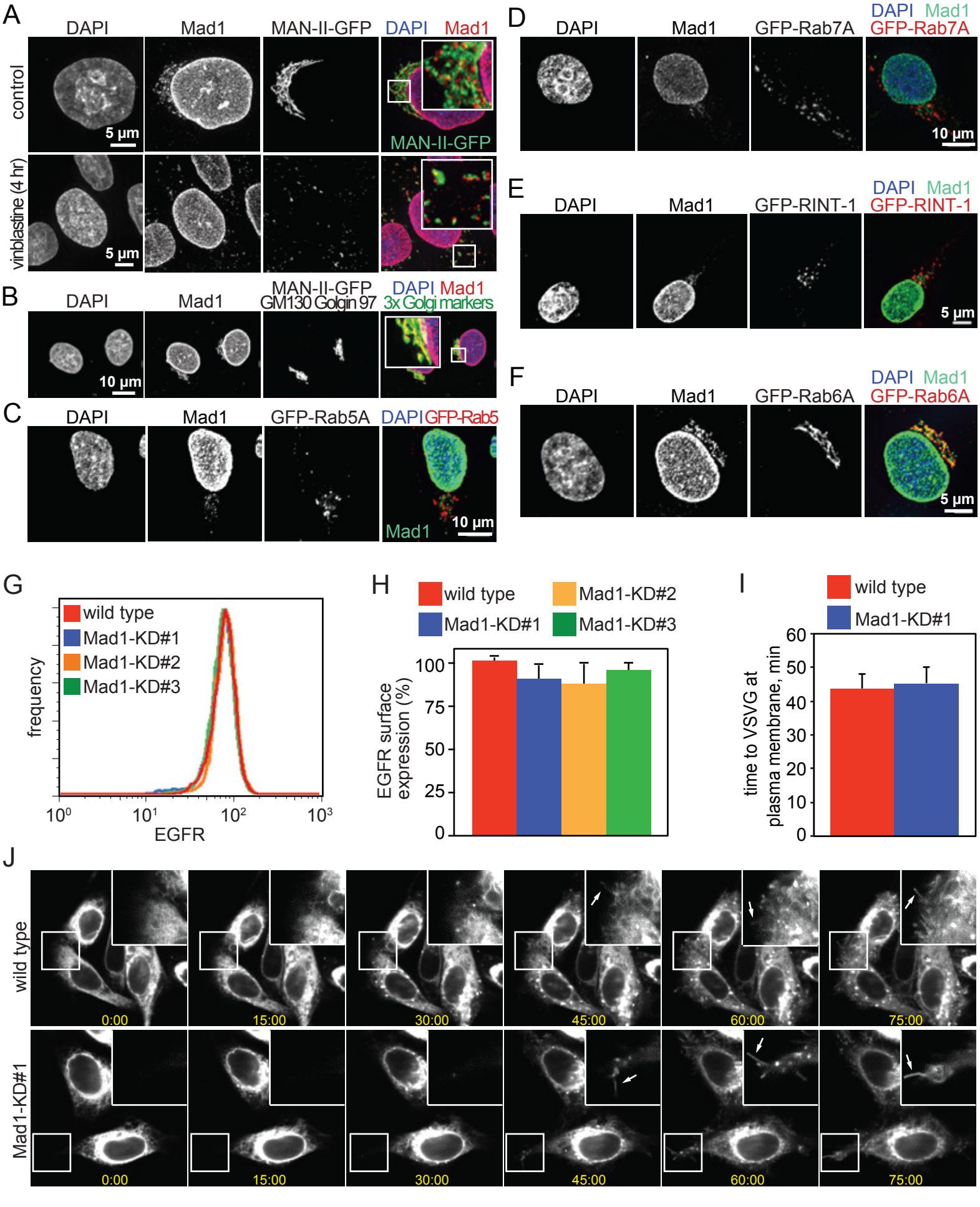
A
DAPI
Mad1
MAN-II-GFP
DAPI Mad1
control
vinblastine (4 hr)
5 μm
MAN-II-GFP
B
DAPI
Mad1
MAN-II-GFP
GM130 Golgin 97
DAPI Mad1
3x Golgi markers
10 μm
C
DAPI
Mad1
GFP-Rab5A
DAPI GFP-Rab5
Mad1
10 μm
D
DAPI
Mad1
GFP-Rab7A
DAPI Mad1
GFP-Rab7A
10 μm
E
DAPI
Mad1
GFP-RINT-1
DAPI Mad1
GFP-RINT-1
5 μm
F
DAPI
Mad1
GFP-Rab6A
DAPI Mad1
GFP-Rab6A
5 μm
G
wild type
Mad1-KD#1
Mad1-KD#2
Mad1-KD#3
frequency
EGFR
H
wild type
Mad1-KD#2
Mad1-KD#1
Mad1-KD#3
EGFR surface expression (%)
I
wild type
Mad1-KD#1
time to VSVG at plasma membrane, min
J
wild type
Mad1-KD#1
0:00
15:00
30:00
45:00
60:00
75:00

Figure S2

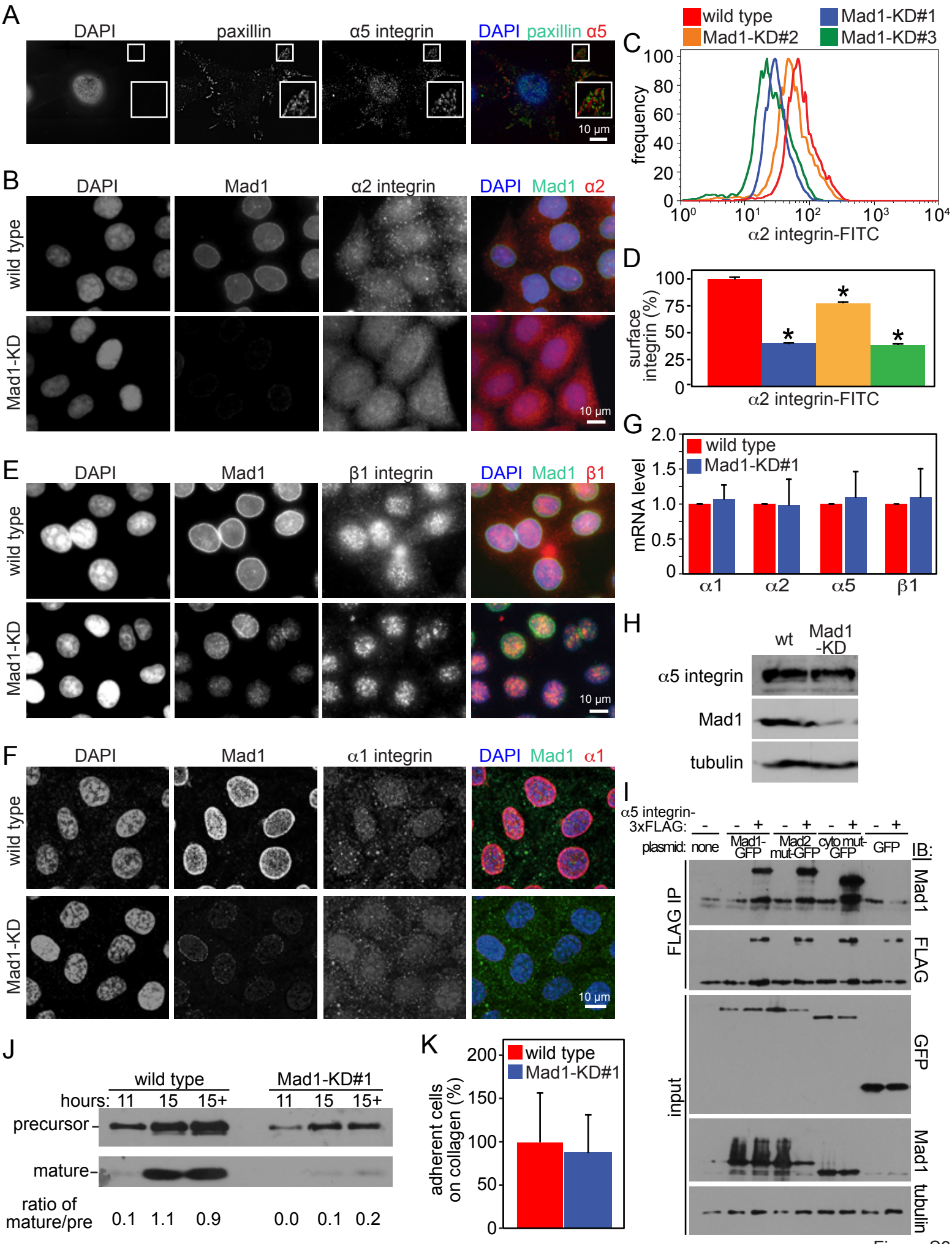
A
DAPI
paxillin
α5 integrin
DAPI paxillin α5
10 μm
B
DAPI
Mad1
α2 integrin
DAPI Mad1 α2
wild type
Mad1-KD
10 μm
C
wild type
Mad1-KD#1
Mad1-KD#2
Mad1-KD#3
frequency
α2 integrin-FITC
D
surface integrin (%)
α2 integrin-FITC
E
DAPI
Mad1
β1 integrin
DAPI Mad1 β1
wild type
Mad1-KD
10 μm
G
wild type
Mad1-KD#1
mRNA level
α1
α2
α5
β1
H
wt
Mad1 -KD
α5 integrin
Mad1
tubulin
F
DAPI
Mad1
α1 integrin
DAPI Mad1 α1
wild type
Mad1-KD
10 μm
I
α5 integrin-3xFLAG:
plasmid: none
Mad1-GFP
Mad2 mut-GFP
cyto mut-GFP
GFP
IB:
FLAG IP
Mad1
FLAG
input
GFP
Mad1
tubulin
J
wild type
Mad1-KD#1
hours: 11 15 15+ 11 15 15+
precursor
mature
ratio of mature/pre
0.1 1.1 0.9 0.0 0.1 0.2
K
wild type
Mad1-KD#1
adherent cells on collagen (%)

Figure S3

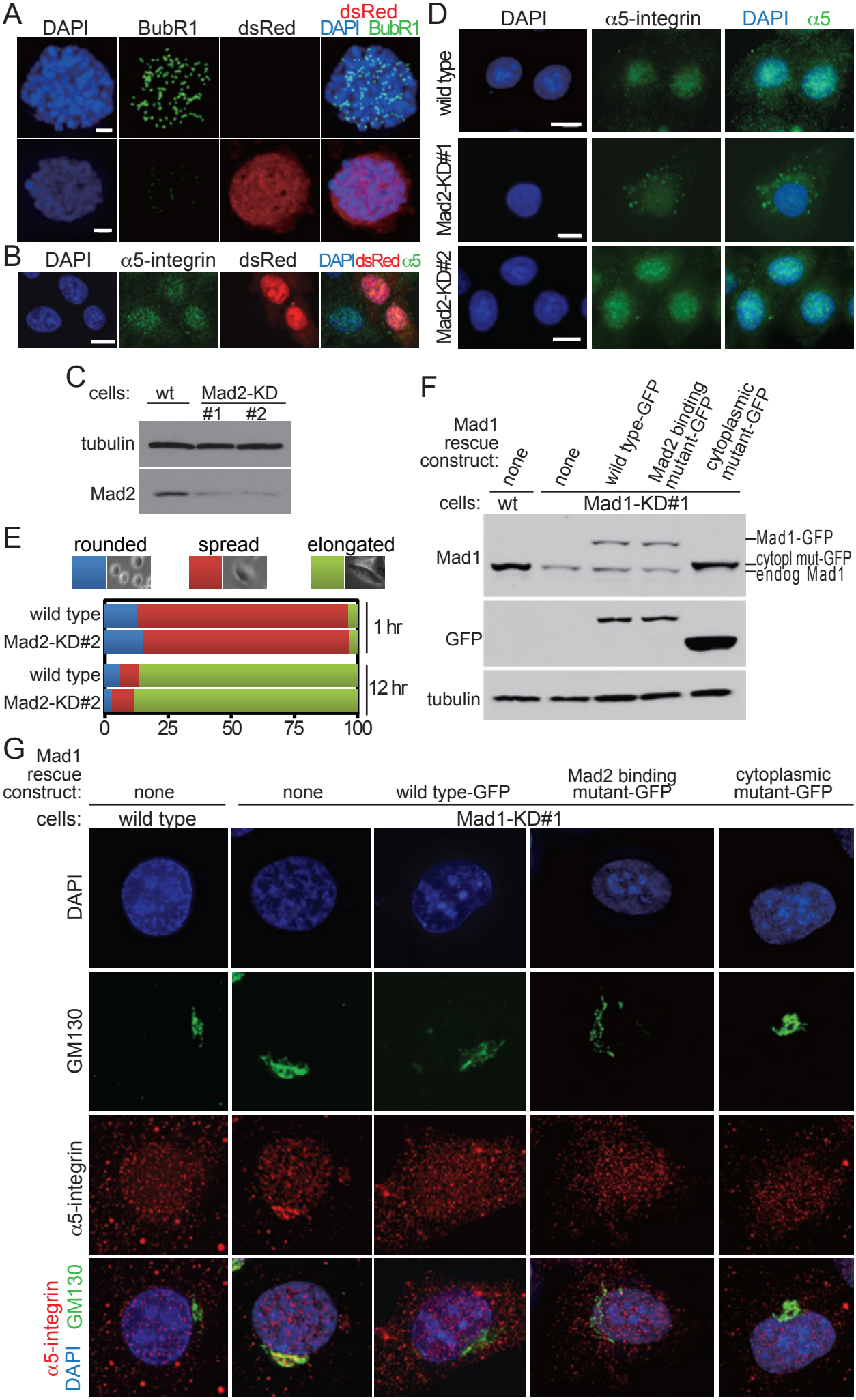
A
DAPI
BubR1
dsRed
dsRed DAPI BubR1
B
DAPI
α5-integrin
dsRed
DAPI dsRed α5
C
cells:
wt
Mad2-KD
#1
#2
tubulin
Mad2
D
DAPI
α5-integrin
DAPI α5
wild type
Mad2-KD#1
Mad2-KD#2
E
rounded
spread
elongated
wild type
Mad2-KD#2
wild type
Mad2-KD#2
1 hr
12 hr
0
25
50
75
100
F
Mad1 rescue construct:
none
none
wild type-GFP
Mad2 binding mutant-GFP
cytoplasmic mutant-GFP
cells:
wt
Mad1-KD#1
Mad1
GFP
tubulin
Mad1-GFP
cytopl mut-GFP
endog Mad1
G
Mad1 rescue construct:
none
none
wild type-GFP
Mad2 binding mutant-GFP
cytoplasmic mutant-GFP
cells:
wild type
Mad1-KD#1
DAPI
GM130
α5-integrin
α5-integrin GM130
DAPI

Figure S4

Supplemental Figure Legends

Figure S1. Identification of a cytoplasmic, perinuclear pool of Mad1 and characterization of Mad1 knockdown cells. Related to Figure 1. (A) Immunofluorescence showing a perinuclear pool of Mad1 in HeLa cells, primary MEFs, and MDA-MB-231 breast cancer cells. The boxed regions are enlarged in the far right panel. (B) Quantification +/- SD of cells exhibiting cytoplasmic localization of Mad1. n = 200 cells from each of 3 independent experiments. (C) Immunoblot of HeLa cell extract showing a complete lane blotted with mouse monoclonal anti-human Mad1 (a kind gift of A. Musacchio) and rabbit polyclonal anti-Mad1 antibody [S1]. (D-E) Fractionation of HeLa cells (D), the human breast cancer cell lines MDA-MB-231 and Cal51 and primary MEFs (E) showing a cytoplasmic portion of Mad1. Histone H3 and lamins A and C were used to show adequate separation of nuclear components from the cytoplasm. Tubulin was used to determine the extent of cytoplasmic protein in the nuclear fraction. (F) siRNA analysis confirms the identity of the cytoplasmic band of Mad1. Fractionation of HeLa cells 3 days after transfection with Mad1-specific or scrambled siRNA. Mad1 in whole cell lysate (WCL), nuclear and cytoplasmic fractions was reduced after siRNA, as detected by both rabbit polyclonal and mouse monoclonal Mad1 antibodies. Histone H3 and lamins A and C were used as nuclear markers. Tubulin was used as a representative cytoplasmic protein. (G-I) Reduction of Mad1 does not cause overt defects in progression through the cell cycle. (G) Flow cytometry analysis of DNA content demonstrating that depletion of Mad1 does not lead to cell cycle delay. (H) Analysis of mitotic index +/- SD in asynchronously cycling HeLa cells based on microscopic analysis of DNA and tubulin staining. Partial depletion of Mad1 does not affect the percentage of untreated cells in mitosis. (I) Growth curves +/- SD showing that there is no proliferation defect in populations of cells expressing reduced levels of Mad1. (J) Analysis of Mad1 expression in control HeLa cells and three lines constitutively expressing Mad1-specific shRNA in which the level of Mad1 is knocked down (Mad1-KD#1-3). Each Mad1-KD cell lines expresses a distinct shRNA sequence. (K) The nuclear fraction of Mad1 is reduced, but still present, in Mad1-KD cell lines #1-3, whereas the cytoplasmic fraction of Mad1 becomes undetectable. Arrows indicate the cytoplasmic portion of Mad1 in HeLa cells expressing wild type levels of Mad1. (L) All fractions of Mad1 are reduced in Mad1-KD stable knockdown cells, as assessed by both mouse and rabbit anti-Mad1 antibodies. Tubulin, cytoplasmic marker. Lamin A/C and histone H3, nuclear markers. (M) A portion of Mad1-YFP is cytoplasmic. 48 hours after transient transfection with pcDNA5-Mad1-YFP, HeLa cells were harvested, fractionated, and analyzed as in D-F.

Figure S2. Cytoplasmic Mad1 localizes to the Golgi, but is not required for global secretion. Related to Figure 2. (A) Perinuclear cytoplasmic Mad1 staining in HeLa cells is dispersed after 4 hours of 100 ng/mL vinblastine, as is the Golgi protein MAN-II-GFP. The boxed regions are enlarged in the insets. (B) Near complete colocalization of cytoplasmic Mad1 with the Golgi markers MAN-II, GM130 and Golgin 97, all of which are shown in green in the merged image. The boxed region is enlarged in the inset. (C-F) HeLa cells were transiently transfected with

the early endosome marker GFP-Rab5A (C), the late endosome marker GFP-Rab7A (D), GFP-RINT-1 (E), which cycles between the Golgi and the ER, or GFP-Rab6A (F), which localizes to endosomes and to the trans Golgi. 36 hours after transfection, cells were processed for immunofluorescence and examined for colocalization with Mad1. Cytoplasmic Mad1 partially colocalizes with Rab6A. (G-H) EGFR localization on the cell surface is unaffected by reduction of Mad1 in three distinct Mad1 knockdown lines. (G) Flow cytometry analysis of surface expression of EGFR. (H) Quantification +/- SEM of surface expression of EGFR as measured in G. n=10,000 events from each of 3 independent experiments. (I-J) Secretion of VSVG is not delayed by reduction of Mad1. 24 hours after transfection of VSVG-GFP, wild type and Mad1-KD#1 HeLa cells were incubated overnight at 42°C to cause VSVG-GFP to misfold and accumulate in the ER. Cells were imaged at 32°C to allow proper folding and secretion of VSVG-GFP. (I) Quantitation +/- SD of the time after shift to 32°C required for appearance of VSVG-GFP on the plasma membrane. n=5. (J) Still images from timelapse analysis of VSVG-GFP secretion. Insets show an enlarged view of boxed regions on the cell periphery. Arrows indicate localization of VSVG-GFP to plasma membrane protrusions. Time is shown in minutes:seconds. See also Supplemental Movie S1.

Figure S3. α1, α2 and β1 integrin do not accumulate substantially in the Golgi after Mad1 depletion. Related to Figure 2. (A) A single z plane from the bottom of a wild type HeLa cell showing α5 integrin colocalizes with focal adhesions, labeled with paxillin. (B-F) Although their localization in Mad1-KD#1 cells is distinguishable from their localization in wild type HeLa cells, neither α2 integrin (B), β1 integrin (E), nor α1 integrin (F) accumulate substantially at the periphery of the nucleus in Mad1-KD cells, unlike α5 integrin (Fig. 2A-C). Single z planes from the center of the cells are shown. (C) Flow cytometry analysis of surface expression of α2 integrin demonstrates a deficit in α2 integrin secretion that is not as severe as that for α5 integrin (Fig. 2D-E). (D) Quantification of surface expression of α2 integrin as measured in C. n=10,000 events from each of 2 independent experiments. (E) Two cells that unusually retained near normal levels of Mad1 expression in the Mad1-KD#1 cell line were shown to include an internal control on the same coverslip. (G) mRNA levels of integrins are unaffected by reduction of Mad1. n=2. (H) Immunoblot showing α5 integrin levels in wild type (wt) and Mad1-KD#1 cells. (I) Extracts from HeLa cells transfected with the indicated constructs were immunoprecipitated using beads coupled to anti-FLAG antibodies. Wild type Mad1-GFP, as well as the Mad2-binding deficient mutant and the mutant restricted to the cytoplasm, coimmunoprecipitate with α5 integrin-3xFLAG. (J) Maturation of α5 integrin is impaired in Mad1 knockdown cells. Extracts from HeLa cells transfected with a plasmid expressing α5 integrin-3xFLAG were blotted with anti-FLAG antibodies at 11 and 15 hours after transfection. 15+ indicates cells harvested 15 hours after transfection that received 4 hours of MG132 treatment. α5 integrin-3xFLAG was less well expressed in Mad1 knockdown cells for unknown reasons. However, the ratio of the 18 kD mature C-terminal fragment to the 120 kD precursor is clearly reduced in Mad1-KD#1 cells, demonstrating a deficit in

maturation. Quantitation of the ratio of the mature to the precursor forms is shown below the blot. There is an empty lane in between the wild type and Mad1-KD#1 samples. (K) Mad1 is not required for cellular attachment on collagen. Wild type and Mad1-KD#1 HeLa cells were plated on 40 μg/mL collagen and allowed to attach at 37°C for 30 minutes. The average number of attached cells +/- SD is shown. p=0.1931. n=3.

Figure S4. Mad1 exerts interphase, cytoplasmic effects on α5 integrin secretion that are independent of Mad2. Related to Figure 3. (A-B) Reduction of the mitotic checkpoint component BubR1 does not impair α5 integrin secretion. (A) Immunofluorescence showing depletion of BubR1 in HeLa cells cotransfected with dsRed and siRNA against BubR1, bottom. The top row shows an untransfected cell from the same coverslip. Scale bars, 2.5 μm. (B) α5 integrin does not accumulate in a perinuclear region in cells cotransfected with BubR1 siRNA and dsRed. Scale bar, 10 μm. (C-E) Depletion of the mitotic checkpoint protein and Mad1 binding partner Mad2 does not impair secretion of α5 integrin or cellular spreading on fibronectin. (C) Immunoblot showing reduced levels of Mad2 in two cell lines stably expressing distinct shRNA sequences targeting Mad2. (D) α5 integrin does not accumulate perinuclearly in Mad2 knockdown cell lines. Scale bars, 10 μm. (E) Mad2 knockdown does not cause defects in cellular spreading on fibronectin. (F-G) GFP-tagged wild type Mad1 as well as a GFP-tagged Mad2 binding mutant (K541A/L543A) and a GFP-tagged cytoplasmic mutant lacking the nuclear import signal (aa 180-718) rescue the secretion of α5 integrin. (F) Immunoblot showing expression of GFP-tagged shRNA resistant Mad1 and Mad1 mutants. (G) Immunofluorescence showing α5 integrin no longer accumulates perinuclearly in Mad1 knockdown cells expressing shRNA resistant wild type Mad1 tagged with GFP or the Mad2-binding or cytoplasmic mutants of Mad1 tagged with GFP.

Supplemental Experimental Procedures

Cell culture

HeLa cells were grown in DMEM with 10% FBS, 100 U/ml penicillin and 100 mg/mL streptomycin and cultured in 5% CO_2 at 37°C. siRNA sequences [S2] were prepared and introduced into HeLa cells by Lipofectamine 2000 as per the manufacturer (Invitrogen). Virus expressing shRNA against Mad1 (5'-AGCGATTGTGAAGAACATG-3' for Mad1-KD#1, 5'-GCTTGCCTTGAAGGACAAG-3' for Mad1-KD#2, 5'-GCGATTGTGAAGAACATGA-3' for Mad1-KD#3) was made from pSUPERIOR.retro.puro. pSUPERIOR.retro.puro containing shRNA sequence against Mad2 (5'-GATGAAATCCGTTCAGTGA-3' for Mad2-KD#1, 5'-GTGGCATATATCCATCTGA-3' for Mad2-KD#2) was transfected into HeLa cells. Stable integrants were selected with 2 μg/mL puromycin. Single clones were isolated with cloning cylinders. Transient depletion of BubR1 was accomplished by transient transfection of a pSuper plasmid co-expressing dsRed and shRNA against BubR1 (5′-AGATCCTGGCTAACTGTTC-3′) [S3]. 60 hours after transfection, cells were treated +/- 100 ng/mL colcemid for 4 hours before analysis.

MDA-MB-231 cells were grown in DMEM with 10% FBS supplemented with 100 U/mL penicillin and 100 mg/mL streptomycin and cultured in 10% CO_2 at 37°C. Human Mad1-YFP in the pcDNA/FRT/TO vector was integrated into MDA-MB-231 cells, which were also modified to contain a single FRT site and express the Tet repressor, by cotransfection with the Flp recombinase. Transfected cells were selected with 400 μg/mL hygromycin. Single clones were isolated with cloning cylinders. Treatment with 1 μg/mL tetracycline was used to induce Mad1-YFP. Unless otherwise specified, vinblastine was used at 100 ng/mL for 12 hours and brefeldin A at 10 μg/mL for 30 minutes.

Antibodies

The polyclonal rabbit anti-human Mad1 antibody (Rb-Mad1) was raised against amino acids 333-617 of human Mad1 [S1]. The mouse monoclonal anti-Mad1 antibody (m-Mad1) was a kind gift from Dr. A. Musacchio and was raised against amino acids 493-713 of human Mad1 [S4]. Additional antibodies used were: Mad2 [S5], monoclonal GM130 (BD Biosciences), α-tubulin (clone DM1A; Sigma), lamin A/C (Upstate), histone H3 (Upstate), monoclonal Golgin 97 (Invitrogen), Ribophorin I [S6], α5 integrin (AbCam), α5 integrin (Santa Cruz) and α2 integrin (AbCam). Antibodies for immunofluorescence to α5 integrin, α2 integrin, monoclonal β1 integrin, monoclonal FAK (all from Millipore), and p-FAK (Y397; Invitrogen), were kind gifts from Dr. P. Keely.

Immunofluorescence and immunoblotting

Cells were rinsed in 37°C PBS, fixed for 7 minutes at 37°C in 4% formaldehyde, and permeabilized for 6 minutes in 0.2% Triton X-100 in PBS. Staining with the p-FAK (Y397) antibody was performed by rinsing cells in PBS and fixing for 6 minutes at −20°C in methanol. Unless otherwise specified, images were acquired on a Nikon Ti-E inverted microscope using a CoolSNAP HQ2 camera driven

by Nikon Elements software and subsequently deconvolved using the AQI 3D Deconvolution module in Nikon Elements. 2D maximum projections assembled in Elements are shown. Overlays were generated in Photoshop. The quantification of p-FAK (Y397) intensity in Fig. 3E was performed on 3D z-stacks using the volume measurement tool in Elements.

For immunoblotting, equal numbers of cells were lysed in 2× sample buffer. Proteins were separated by SDS-PAGE, transferred to nitrocellulose, and probed with antibodies at the same concentrations used for immunofluorescence.

Nuclear and cytoplasmic protein fractionation

To separate nuclear and cytoplasmic extract, high salt isolation of nuclei was carried out using a protocol that was modified from [S7]. Briefly, 1 10 cm dish of approximately 80% confluent HeLa cells was washed twice with PBS. Cells were harvested by trypsin-EDTA and incubated in Buffer A (200 mM HEPES pH 7.9, 400 mM NaCl, 1 mM EDTA, 1 mM EGTA, pH 7.4) with protease inhibitors for 10-15 minutes on ice. NP-40 was added to a final concentration of 0.5%. Lysate was centrifuged at 3000 rpm for 5 minutes to separate supernatant (cytoplasm) and pellet (nuclei).

Subcellular fractionation

To obtain Golgi fractions, four 10 cm dishes of approximately 80% confluent HeLa cells were washed twice in PBS and then once in homogenization buffer (10 mM HEPES–KOH pH 7.5, 0.25 M sucrose and 1 mM EDTA). The cells were collected, suspended in 1 mL of homogenization buffer and then homogenized with 20 strokes in a stainless-steel homogenizer. Lysate was centrifuged at 3000 rpm for 5 minutes to obtain the supernatant. The supernatant fraction was suspended and layered onto a 0–28% OptiPrep (Sigma, D1556) gradient and centrifuged at 5 X 10^4 x g for 10 hours. After centrifugation, 22 0.2 mL fractions were collected from top to bottom.

Plasma membrane stripping

Cell surface proteins were digested as in [S8]. Parental HeLa cells or Mad1-KD cells were grown in a 10 cm dish to 50% confluence and serum starved for 24 hours. Cells were harvested with 0.05% trypsin (w/v), pelleted at 1500 rpm for 5 minutes, washed with PBS at 4°C, and resuspended in 5 mL of PBS at 4°C supplemented with 10 mM DTT, 1 mM EDTA and 1 mM EGTA. Samples were treated with Proteinase K (500 μg/mL) for 30 minutes on ice. The reaction was stopped with a 5 minute incubation with 2 mM PMSF on ice. Cells were washed in DMEM, allowed to recover at 37°C for the indicated amount of time and plated on fibronectin-coated dishes for 30 minutes before scoring adherent cells.

Flow cytometry

To measure integrin expression, 24 hours after seeding 2 x 10^5 wild type and Mad1-KD HeLa cells in 6 well plates, cells were fixed with 1% paraformaldehyde in PBS for 15 minutes, and then blocked in 10% FBS in PBS for 30 minutes. Cells were incubated with 1 μg of control mouse IgG (Sigma), or monoclonal antibodies to α2

or α5 integrins for 60 minutes at room temperature. After washing, the cells were labeled with FITC-conjugated goat anti mouse secondary antibodies for 30 minutes. After washing again, the cells were collected with a cell scraper. 10,000 events were analyzed per experiment.

To measure EGFR secretion, 24 hours after seeding 3 x 10^5 wild type and Mad1-KD HeLa cells in 6 cm plates, cells were removed with trypsin and centrifuged at 300 x g for 5 minutes. Cells were then resuspended in cold DPBS + 1% FBS and incubated with 1 μg of control mouse IgG (Sigma) or monoclonal antibody to EGFR, (NeoMarkers, EGFR Ab-5 (H11)) on ice for 30 minutes. After washing, the cells were labeled with anti-mouse 488 secondary antibody for 30 minutes on ice. After washing again, the cells were resuspended in 300 μL DPBS + 1% FBS. 10,000 events were analyzed using a FACS Calibur.

qRT-PCR

RNA was isolated from HeLa cells using Trizol and reverse transcribed (iScript, Biorad). 25μL reactions containing 300 nM forward and reverse primers and 1x IQ SYBR Green Supermix (Biorad) were annealed at 60°C. GAPDH was used as an internal control. Melting curves were performed at the end of each experiment to confirm amplification of single products. Relative mRNA levels were calculated using the $\Delta\Delta C_t$ method [S9]. Primers used were as in [S9]; for integrin α1: forward 5'- GGTTCCTACTTTGGCAGTATT-3'; reverse 5'-AACCTTGTCTGATTGAGAGCA-3'. Primers for integrin α2 were: forward 5'-GGAACGGGACTTTCGCAT-3'; reverse 5'-GGTACTTCGGCTTTCTCATCA-3'. Primers for integrin α5 were: forward 5'-TGCAGTGTGAGGCTGTGTACA-3'; reverse 5'-GTGGCCACCTGACGCTCT-3'. Primers for integrin β1 were: forward 5'-GAAGGGTTGCCCTCCAGA-3'; reverse 5'-GCTTGAGCTTCTCTGCTGTT-3'.

Cell adhesion assay

The cell adhesion assay was performed as described previously [S10]. Briefly, each well of a 24 wellplate was coated with 5 μg/mL fibronectin for 1 h at 37°C. After overnight serum starvation, control and Mad1-KD HeLa cells were harvested with trypsin/EDTA, counted with a hemocytometer and resuspended in DMEM. 2 x 10^5 cells were added to each well and allowed to adhere for 30 minutes at 37°C. After incubation, non-attached cells were removed by three gentle washes with DMEM, and the attached cells were fixed before counting. At least 10 randomly selected fields for each cell line were counted to obtain an average cell number per field.

Transwell assay

12 well transwell chambers (Corning) were used to monitor tumor cell migration. The underside of the polycarbonate membrane was coated overnight in 5 μg/mL fibronectin and air dried. Cells were cultured in 0.1% FBS for 24 hours and then trypsinized and added to the upper chambers at 2 x 10^5 cells per transwell with an 8 μm pore size membrane in FBS free medium with 0.1% BSA. Growth medium containing 20% FBS was placed in the lower chamber of the transwell

chamber. After a 6 hour incubation (for MDA-MB-231 cells) or a 22 hour incubation (for HeLa cells), cells on the upper side of the membrane were removed by wiping with a cotton swab. Migrated cells were fixed in methanol and stained with crystal violet. To quantify the number of migrated cells, five random images were taken at 10x magnification and counted using Image J software.

Cell spreading and wound healing assays

For observing cell spreading, HeLa cells were serum starved overnight and trypsinized with 0.05% trypsin/EDTA for 5 minutes, centrifuged, resuspended in DMEM (without FBS) and placed on a glass bottom dish coated with 5 μg/mL of fibronectin (Sigma) for 60 minutes at 37°C. Cell spreading was recorded by phase contrast microscopy every 5 minutes for 12 hours using a 40x, 0.75 NA objective on a Nikon Ti-E microscope equipped with an environmental chamber at 37°C containing 5% CO_2.

For the wound healing assay, 6 well plates coated with 5 μg/mL fibronectin at 37°C for 1 hour were washed with PBS. Cells were trypsinized, centrifuged, and 15–20 × 10^5 cells were seeded and cultured overnight. After rinsing with PBS, cells were incubated in DMEM with 0.1% serum for 12 hours. A 200 μL pipet tip was used to create the "wound", and cells were rinsed with PBS and fed with complete culture medium supplemented with 10% FBS. The wounds were imaged by phase contrast microscopy every 5 minutes using a 10x, 0.3 NA objective. Healing was quantified by manually measuring the wound areas that remained using Elements software. Migrated cells were counted from at least 5 randomly selected areas. Each experiment was reproduced at least in triplicate for each cell type.

VSVG secretion assay

4 hours after plating at 20% confluency, wild type and Mad1-KD#1 cells were transfected using 2 μg of pcDNA/FRT/TO/VSVG-GFP plasmid DNA and 6 μL of FuGENE HD in 400 μL of Optimem. After 24 hours, cells were moved to 42°C overnight to induce misfolding and ER accumulation of VSVG-GFP. Cells were transferred to CO_2 independent media with 10 μg cycloheximide 3 hours before imaging. Imaging occurred at the permissive temperature of 32°C to permit proper folding and secretion of VSVG-GFP. Images were acquired every minute on a swept-field confocal microscope (Nikon Ti-E) using a 60x 1.4NA objective and perfect focus at 10% laser power with 400 ms exposures for 3.5 hours. Acquisition parameters were controlled by Nikon Elements software, and image analysis was conducted using Metamorph software.

Single cell migration assay

Following established soft lithography methods [S11], PDMS straight microchannels (with surface area 5 mm^2, and a channel volume of 0.75 μL, see image below) were fabricated in a Microtechnology Medicine Biology lab.
After being seeded into the micro channels, HeLa cells were allowed to attach and adhere in media containing 0.1% FBS for 12 hours. 20% FBS, as a chemical trigger and stimulus for migration, was then added into the large output. Phase contrast images were taken every 5 minutes using a 10x objective on a Nikon Ti-E inverted

microscope driven by Nikon Elements software for 14 hours. The cell migration data was calculated using an established platform, Je'Xperiment (JEX), following the cell migration tracking protocol [S12]. This platform identifies and tracks the position of each single cell over the time of culture, and performs calculations to estimate the migration distance and speed for both single cells and regions of interest.

Statistical analysis

Significant differences were determined using a two-tailed Student t test. Results are presented as mean ± SD unless otherwise specified.

Supplemental References

S1. Ryan, S.D., Britigan, E.M., Zasadil, L.M., Witte, K., Audhya, A., Roopra, A., and Weaver, B.A. (2012). Up-regulation of the mitotic checkpoint component Mad1 causes chromosomal instability and resistance to microtubule poisons. Proc Natl Acad Sci U S A *109*, E2205-2214.

S2. Martin-Lluesma, S., Stucke, V.M., and Nigg, E.A. (2002). Role of Hec1 in spindle checkpoint signaling and kinetochore recruitment of Mad1/Mad2. Science *297*, 2267-2270.

S3. Kops, G.J., Foltz, D.R., and Cleveland, D.W. (2004). Lethality to human cancer cells through massive chromosome loss by inhibition of the mitotic checkpoint. Proc Natl Acad Sci U S A *101*, 8699-8704.

S4. De Antoni, A., Pearson, C.G., Cimini, D., Canman, J.C., Sala, V., Nezi, L., Mapelli, M., Sironi, L., Faretta, M., Salmon, E.D., et al. (2005). The Mad1/Mad2 complex as a template for Mad2 activation in the spindle assembly checkpoint. Curr Biol *15*, 214-225.

S5. Kops, G.J., Kim, Y., Weaver, B.A., Mao, Y., McLeod, I., Yates, J.R., 3rd, Tagaya, M., and Cleveland, D.W. (2005). ZW10 links mitotic checkpoint signaling to the structural kinetochore. J Cell Biol *169*, 49-60.

S6. Schindler, A.J., and Schekman, R. (2009). In vitro reconstitution of ER-stress induced ATF6 transport in COPII vesicles. Proc Natl Acad Sci U S A *106*, 17775-17780.

S7. Rosner, M., and Hengstschläger, M. (2008). Cytoplasmic and nuclear distribution of the protein complexes mTORC1 and mTORC2: rapamycin triggers dephosphorylation and delocalization of the mTORC2 components rictor and sin1. Hum Mol Genet *17*, 2934-2948.

S8. Martel, V., Vignoud, L., Dupé, S., Frachet, P., Block, M.R., and Albigès-Rizo, C. (2000). Talin controls the exit of the integrin alpha 5 beta 1 from an early compartment of the secretory pathway. J Cell Sci *113 (Pt 11)*, 1951-1961.

S9. Dingemans, A.M., van den Boogaart, V., Vosse, B.A., van Suylen, R.J., Griffioen, A.W., and Thijssen, V.L. (2010). Integrin expression profiling identifies integrin alpha5 and beta1 as prognostic factors in early stage non-small cell lung cancer. Mol Cancer *9*, 152.

S10. Riggs, K.A., Hasan, N., Humphrey, D., Raleigh, C., Nevitt, C., Corbin, D., and Hu, C. (2012). Regulation of integrin endocytic recycling and chemotactic cell migration by syntaxin 6 and VAMP3 interaction. Journal of cell science *125*, 3827-3839.

S11. Duffy, D.C., McDonald, J.C., Schueller, O.J., and Whitesides, G.M. (1998). Rapid Prototyping of Microfluidic Systems in Poly(dimethylsiloxane). Anal Chem *70*, 4974-4984.

S12. Sackmann, E.K., Berthier, E., Young, E.W., Shelef, M.A., Wernimont, S.A., Huttenlocher, A., and Beebe, D.J. (2012). Microfluidic kit-on-a-lid: a versatile platform for neutrophil chemotaxis assays. Blood *120*, e45-53.